ICHEP'98 #122
Submitted to Pa 1, 9
Pl 1, 10, 11

DELPHI 98-120 CONF 181
9 July, 1998

Measurement of the Z Partial Decay Width into $c\bar{c}$ and Multiplicity of Charm Quarks per b Decay

Preliminary

DELPHI Collaboration

D. Bloch[1], **Th. Brenke**[2], **L. Chaussard**[3],
M. Elsing[4], **J.-P. Engel**[1], **P.Sponholz**[2]

Abstract

The partial decay width R_c of the Z into $c\bar{c}$ quark pair and the number of charm quarks n_c per b decay are measured with the DELPHI detector at LEP. Particle identification provided by the Ring Imaging Cherenkov counters and the Time Projection Chamber is used to obtain clear D^0, D^+, D_s^+ and Λ_c^+ signatures. The charm hadron production rate is measured in each channel from a fit of the scaled energy, impact parameter information and the invariant mass spectrum from which R_c and n_c are inferred:

$$\begin{aligned} R_c &= 0.1699 \pm 0.0049(stat) \pm 0.0096(syst) \pm 0.0078(Br) \\ n_c &= 1.172 \pm 0.031(stat) \pm 0.070(syst) \pm 0.052(Br)\,. \end{aligned}$$

Paper submitted to the ICHEP'98 Conference
Vancouver, July 22-29

[1] Institut de Recherches Subatomiques, Strasbourg, France
[2] Bergische Universität – Gesamthochschule Wuppertal, Germany
[3] Institut de Physique Nucléaire, Lyon, France
[4] CERN, Geneva, Switzerland

1 Introduction

A precise determination of the partial decay width R_c of the Z into $c\bar{c}$ quark pairs provides a fundamental test of the Standard Model. The measurement of the number of charm quarks n_c per b decay is an important input to resolve the discrepancy between the experimental value of $BR(b \to l\nu X)$ and its theoretical prediction [1]. In this paper a simultaneous measurement of these quantities via the charm counting technique [2] is presented. The measured rate of D or Λ hadrons in $b\bar{b}$ and $c\bar{c}$ events is given by twice the product of the partial width $R_{c(b)}$ times the probability $P_{c(b)\to D,\Lambda}$ of the quark to produce a given charm hadron. For $c\bar{c}$ events the sum over the probabilities $P_{c\to D,\Lambda}$ for all weakly decaying charm hadrons adds up to one. Hence R_c can be extracted from the sum of the rates. In $b\bar{b}$ events the sum of the production probabilities is a direct measurement of the number of charm quarks n_c per b decay. The large number of events collected at LEP I leads to significant improvements in the precision compared to previous DELPHI results [4].

Since charm hadrons are produced both in $c\bar{c}$ and $b\bar{b}$ events, the separation between these flavors is necessary. A fit of the simulated b and c contributions to the measured impact parameter information, scaled energy $X_E = 2E_D/\sqrt{s}$ and invariant mass spectrum is used to separate the classes. In this analysis charm hadrons are reconstructed in the following decay modes [1]:

- $D^0 \to K^-\pi^+$
- $D^+ \to K^-\pi^+\pi^+$
- $D_s^+ \to \phi(1020)\pi^+$ and $D_s^+ \to \bar{K}^*(892)K^+$
- $\Lambda_c^+ \to pK^-\pi^+$

The combinatorial background is largely reduced by identifying kaons and protons in the charm hadron decay products using particle identification information provided by the DELPHI Ring Imaging Cherenkov Counters (RICH) and the measured specific energy loss in the Time Projection Chamber (TPC).

2 The DELPHI detector

The DELPHI detector consists of several independent devices for tracking, calorimetry, lepton and particle identification. Only the tracking and particle identification components are relevant for this analysis and will be briefly described in the following. A detailed description of the whole apparatus and its performance can be found in [5].

Looking from the interaction point through the detector, the closest tracking device is the Vertex Detector (VD). The LEP I version of the detector was build up from three concentric layers of silicon micro strip modules with the outer layer having 11 cm radius. Since 1994 the single sided closer and outer layer have been replaced by double sided modules. With an intrinsic $R\phi$ resolution of 7.6 μm [5] the VD is the main component to reconstruct secondary vertices of heavy hadron decays. The VD is followed by the Inner

[1] Throughout this paper charge-conjugate states are implicitly included.

Detector (ID) which consists of a jet chamber part and a proportional chamber. The Time Projection Chamber is the main tracking device in DELPHI. Charged particles are measured with a precision of approximately 250 μm in $R\phi$ and 880 μm in z [5]. From the measured amplitudes on up to 192 sense wires the specific energy loss of charge particles (dE/dx) can be measured. The outermost tracking component for the barrel region is the Outer Detector (OD) made out of 5 layers of drift tubes. The DELPHI Barrel RICH is placed between the TPC and the Outer Detector. With its two radiators it is able to identify pions, kaons and protons over nearly the full momentum range.

The charged tracking is extended to the forward region by two wire chambers FCA and FCB. FCA is mounted on the endcap of the TPC and covers a polar angle range from 11° to 32°, while FCB is placed behind the forward RICH on both sides of the DELPHI endcaps. FCB covers the polar angle range from 11° to 36°.

3 Event selection and simulation

Charged particles were selected as follows: the momentum was required between 0.4 GeV/c and 50 GeV/c, the relative error on momentum measurement less than 100%, the polar angle relative to the beam axis between 20° and 160°, the track length in the TPC larger than 30 cm, the projection of the impact parameter relative to the interaction point had to be less than 4 cm in the plane transverse to the beam direction and the distance to the interaction point along the beam direction less than 10 cm.

Hadronic events were selected by requiring five or more charged particles and a total energy in charged particles larger than 12% of the collision energy, assuming all charged particles to be pions. A total of 3.5 million hadronic events was obtained from the 1992-1995 data, at centre-of-mass energies within 2 GeV to the Z resonance mass. According to the simulation, the selection efficiency for hadronic Z decays was 95.7%. The data sample contained also 0.24% of τ pair and 0.19% of Bhabha events. The bias due to this contamination is taken into account in the following. All other background sources were found to be negligible.

For each event, the primary interaction vertex was determined from the measured tracks with a constraint on the measured mean beam spot position. The fit was iterated until either the χ^2/NDF of all contributing tracks was less than 3 or at least two charged particle tracks were left. All track parameters were then redefined after a helix extrapolation to this vertex position. The resolution of tracks measured only by the forward tracking chambers was improved by a track refit using the primary vertex. Tracks having a fit χ^2 larger than 100 were removed from the analysis.

The simulation was done with the JETSET 7.4 Parton Shower model [6] using DELPHI tuned parameters obtained from a fit to event shape distributions and identified particle spectra [7]. The heavy hadron decay tables were modified to include D^{**} and B^{**} production with rates of 30% B^{**} in $b\bar{b}$ events and 30% D^{**} in $c\bar{c}$ events. The fragmentation function used for b and c quarks was that of Peterson et al. [8]:

$$f(z) \propto \left[z \left(1 - \frac{1}{z} - \frac{\epsilon_q}{1-z} \right)^2 \right]^{-1} \qquad (1)$$

where z is the fraction $(E + p_{||})_{hadron}/(E + p_{||})_{quark}$ with $p_{||}$ the momentum component parallel to the quark direction. The $\epsilon_{q=b,c}$ parameters were adjusted in order to reproduce

the average energy fractions $\langle X_E^b(B)\rangle = 0.702 \pm 0.008$ and $\langle X_E^c(D^*)\rangle = 0.510 \pm 0.005 \pm 0.008$ taken by B and D^* hadrons in Z events [9], respectively.

4 Charm hadron reconstruction

Candidates for the charm hadron decays $D^0 \to K^-\pi^+$, $D^+ \to K^-\pi^+\pi^+$, $D_s^+ \to \phi(1020)\pi^+$, $D_s^+ \to \bar{K}^*(892)K^+$ and $\Lambda_c^+ \to pK^-\pi^+$ were reconstructed from all possible combinations of charged particles with a momentum larger than 1 (2) GeV/c for pion and kaon (proton) candidates. For D_s^+ candidates, a minimum momentum of 3 GeV/c was required for the ϕ and $\bar{K}^*$ and the invariant ϕ and $\bar{K}^*$ masses had to lay within $1.01 - 1.03$ GeV/c^2 and $0.86 - 0.94$ GeV/c^2, respectively.

In order to remove badly measured tracks from secondary interactions, all particles associated to the charm hadron candidate were required to have at least one associated VD hit. These tracks were then used to fit a secondary vertex in space and the track parameters were recomputed at this common secondary vertex. Candidates for a given decay were retained if their invariant mass and scaled energy, X_E, satisfied the cuts given in table 1.

Particle	mass (GeV/c^2)	X_E^{min}
D^0	1.80 - 2.20	0.30
D^+	1.70 - 2.05	0.20
D_s^+	1.90 - 2.20	0.20
Λ_c^+	2.10 - 2.50	0.30

Table 1: *Invariant mass range and minimum scaled energy for each channel.*

To reject the combinatorial background a cut on the helicity angle was applied. This quantity, Θ_h, was defined as the angle between the sphericity axis of the decay products in the rest frame of the charm hadron (D or Λ) with respect to its direction of flight. The pseudo-scalar charm ground states decays are isotropic in this angle while the combinatorial background has a clear enhancement at $\cos\Theta_h = \pm 1$. Since the background is concentrated at lower energies than charm hadrons, energy dependent cuts in the helicity angle distribution

$$X_E > a \cdot e^{+b(\cos\Theta_h - 1)} - c \;\text{ and }\; \mathrm{X_E} > \mathrm{a} \cdot \mathrm{e}^{-\mathrm{b}(\cos\Theta_\mathrm{h}+1)} - \mathrm{c} \qquad (2)$$

were used, which decreased in strength with increasing energy. The corresponding coefficients are listed in table 2.

The charm candidate's decay length, ΔL, was calculated as the distance between the primary and the decay vertex in the plane transverse to the beam axis, projected on the charm direction of flight. The sign of the decay length was set negative if the decay vertex was behind the primary vertex w.r.t. the direction of flight. A positive value of ΔL was required in order to remove the combinatorial background due to particles from the primary vertex. To allow for a much lower combinatorial background level at large energies an additional energy dependent decay length cut was introduced:

$$\Delta L(X_E) > x \cdot (X_E - X_E^{min})^2 + y \quad \text{and} \quad \Delta\mathrm{L} > \Delta\mathrm{L_{min}} \qquad (3)$$

Particle	a	b	c
D^0	0.5	2.0	0.20
D^+	0.5	3.0	0.10
D_s^+	0.5	3.0	0.10
Λ_c^+	0.5	3.0	0.15

Table 2: *Energy dependent cut values on the helicity angle.*

with coefficients listed in table 3 for the different decay channels. The value X_E^{min} is the one given in table 1. No energy dependent cut was used for the Λ_c and the $D_s^+(\bar{K}^*)$ sample, for which the best signal to background ratio was obtained with a larger ΔL_{min} value.

Particle	x	y	ΔL_{min} (cm)
D^0	-0.5	0.125	0.050
D^+	-1.0	0.230	0.125
$D_s^+(\phi)$	-1.0	0.100	0
$D_s^+(\bar{K}^*)$	-	-	0.100
Λ_c^+	-	-	0.015

Table 3: *Minimum decay length and parameters for the energy dependent decay length cut.*

For the $D_s^+(\phi)$ sample an additional selection was applied on the angle $\Theta_{K\pi}$ between one of the kaons from the ϕ and the remaining pion in the rest frame of the ϕ. This angle follows a $\cos^2(\Theta_{K\pi})$ distribution because of the spin structure of the decay, while the background is flat. A cut on $\cos(\Theta_{K\pi}) > 0.3$ was used for the $D_s^+(\phi)$ sample, whereas the $D_s^+(\bar{K}^*)$ sample showed no significant improvement with such a cut.

Another kinematical quantity used to remove the background was the χ^2 probability, $\mathcal{P}(\chi^2)$, at the secondary vertex. For well measured secondary vertices the probability is flat between 0 and 1, while it peaks at 0 for bad combinations. For the D^+ and Λ_c^+ decay modes a cut of $\mathcal{P}(\chi^2) > 0.001$ is used, while a tighter cut of 0.01 is applied in some years for both D_s^+ channels. The breakdown of the probability cuts for the D_s^+ channels can be found in table 4. No cut was applied on the two body decay vertex of the D^0.

Particle	1992	1993	1994	1995
$D_s^+(\phi)$	0.001	0.01	0.001	0.001
$D_s^+(\bar{K}^*)$	-	0.001	0.01	0.001

Table 4: *Cuts on the secondary vertex χ^2 probability for the D_s^+ channels.*

The particle identification provided by the RICH and the specific energy loss dE/dx measurement in the TPC were used to identify kaon and protons. To illustrate the

performance of the particle identification, a $D^{*+} \to D^0\pi^+$ sample is used to obtain a high purity kaon and pion sample from the $D^0 \to K^-\pi^+$ decay . The response from the RICH gas and liquid radiators on this sample is shown in figure 1. The same sample is used in figure 2 to show the measured energy loss of kaons and pions at energies larger than 1.5 GeV.

The tagging of the kaons and protons from the charm hadron decays was done using DELPHI standard tagging routines for the RICH [10] and the dE/dx [5] identification. For the RICH, the measured Cherenkov angle information was translated into π, K and p tagging words. The dE/dx information was only used if no RICH information was available. Here the tagging was done using the *pull* of the measured dE/dx w.r.t. the expected value for a given particle type. For all ground state decay modes except the D^0 a candidate kaon or proton was rejected if no RICH or dE/dx identification was available.

The D^0, D^+, D_s^+, Λ_c^+ obtained after these selections are shown in figures 3 to 7. Because of the small amount of available RICH information, the 1992 data are not used for the $D_s^+(\bar{K}^*)$ and Λ_c^+ sample. The reflections from other D decay modes are shown as the dotted lines. D^+ decays into $K^-K^+\pi^+$ or $K^-\pi^+\pi^+$, where the wrong mass is assigned to one of the pions, is an important background in the D_s^+ spectrum, as can be seen in figures 5 and 6. An additional cut is applied to the D^+ sample in order to remove the background from $D^{*+} \to D^0\pi^+$ decays, where the D^0 decays into $K^-\pi^+$. The difference between the $K^-\pi^+\pi^+$ and any of the $K^-\pi^+$ combinations had to be larger than 150 MeV/c^2.

5 Fit method

For a measurement of R_c and n_c it is necessary to distinguish the charm production in $c\bar{c}$ and $b\bar{b}$ events in an optimal way in order to keep correlations small. To achieve the best separation, the scaled energy of the charm hadron was used together with the impact parameter b-tag [12] in a combined fit.

The impact parameter information of each charged particle track was used to define the probability $\mathcal{P}_{ev}$ that all tracks were compatible with a common primary vertex [12]. Since the distribution peaked around zero for $b\bar{b}$ events, a transformation

$$tr(\mathcal{P}_{ev}) = \frac{4}{4 - ln(\mathcal{P}_{ev})} \tag{4}$$

was applied to stretch this area. The selection of charm hadrons resulted in a sample of events with tracks having large impact parameters, especially for the D^+ sample because of its long lifetime. Hence $\mathcal{P}_{ev}$ was computed only from particles in the event which were not associated to the charm hadron candidate.

The X_E distribution was used because charm hadrons from $c\bar{c}$ events have a harder energy spectrum than those coming from B decays. Combining both variables allows to separate the background form light quark events from $b\bar{b}$ and $c\bar{c}$ events. Light quark events are expected to have large $tr(\mathcal{P}_{ev})$ and small X_E, while both other classes are either concentrated at small $tr(\mathcal{P}_{ev})$ or large X_E.

The charm hadron X_E and $tr(\mathcal{P}_{ev})$ distributions for the different decay modes are shown in figures 8 to 17. The combinatorial background is subtracted from the data using a fit of the Monte Carlo background to the sidebands of the signals. No correction

for the reconstruction efficiency is applied. The Monte Carlo rates of charm hadrons in $c\bar{c}$ and $b\bar{b}$ events are scaled with the final fit results.

Particle	$mass$	X_E	$tr(\mathcal{P}_{ev})$	$\langle N^{dat}_{i,j,k} \rangle$
D^0	10	5	5	244
D^+	10	6	6	218
$D_s^+(\phi)$	10	5	5	21
$D_s^+(K^*)$	8	5	5	19
Λ_c^+	10	5	5	28

Table 5: *Number of bins used in each dimension and the average number of events per bin.*

The fit of the charm hadron rates $R_q \cdot P_{q\to X} \cdot BR$ in $c\bar{c}$ and $b\bar{b}$ events was binned in three dimensions of invariant mass, X_E and $tr(\mathcal{P}_{ev})$. The number of bins in each dimension and the average number of data events per bin are listed in table 5. The width of each bin was chosen to keep the number of events per bin about constant. The fit was done with two different approaches depending on the average number of entries per bin. For the D^0 and D^+ this number was around 230. Therefore a χ^2 fit was performed:

$$\chi^2 = \sum_i^{mass} \sum_j^{tr(\mathcal{P}_{ev})} \sum_k^{X_E} \left(\frac{N^{dat}_{i,j,k} - \lambda_{i,j,k}}{\sigma_{i,j,k}} \right)^2 . \tag{5}$$

Here $N^{dat}_{i,j,k}$ is the number of data events in a given bin, $\sigma_{i,j,k}$ is the quadratic sum of the statistical error of the data and the Monte Carlo prediction. The expected number of events $\lambda_{i,j,k}$ is calculated assuming the Monte Carlo shape from the different classes. $\lambda_{i,j,k}$ is given by:

$$\begin{aligned} \lambda_{i,j,k} &= \frac{2N_{had}}{\epsilon_{had}} \sum_{q=b,c,g\to c\bar{c}} R_q \cdot P_{q\to X} \cdot BR \cdot \frac{\epsilon_{i,j,k} N^{signal}_{i,j,k}(q)}{N^{signal}_{tot}(q)} \\ &\quad + N^{back}_{i,j,k} \cdot n^{back}_{j,k} + N^{reflect}_{i,j,k} . \end{aligned} \tag{6}$$

The first term of this equation reflects the charm hadron signal with its contributions from $b\bar{b}$, $c\bar{c}$ and light quark events. The ratio $N^{signal}_{i,j,k}(q)$ over $N^{signal}_{tot}(q)$ denotes the flavour dependent shape of the signal in the Monte Carlo including the reconstruction efficiency $\epsilon_{i,j,k}$. N_{had} is the total number of hadronic events and ϵ_{had} their selection efficiency.

The second term describes the Monte Carlo background shape. Here the $N^{back}_{i,j,k}$ rates include an overall normalisation obtained from a fit of the Monte Carlo invariant mass spectra to the data in the sidebands of the signal. The $n^{back}_{j,k}$ are additional background normalisations for each bin in X_E and $tr(\mathcal{P}_{ev})$. They are introduced to allow for little fluctuations in the Monte Carlo background description.

The rate of charm hadrons from $b\bar{b}$ and $c\bar{c}$ events $R_q \cdot P_{q\to X} \cdot BR$ as well as the background normalisation $n^{back}_{j,k}$ in each bin in X_E and $tr(\mathcal{P}_{ev})$ were free parameters in the fit. The rate of charm hadrons in light quark events was determined by the rate of gluon splitting into heavy quarks [9].

Figure 18 shows the background normalisations as determined in the fit for the D^0 and D^+ where 5×5 and 6×6 separating bins in X_E and $tr(\mathcal{P}_{ev})$ have been chosen, respectively. The mean values are 0.978 and 0.969, the RMS is 0.096 and 0.097, respectively. Since the overall normalisation of the combinatorial background should be preserved, an additional term was added to the overall χ^2:

$$\chi^2 = \left(\frac{R-1}{\sigma_R}\right)^2 \tag{7}$$

with

$$R = \frac{\sum_i^{mass}\sum_j^{tr(\mathcal{P}_{ev})}\sum_k^{X_E} N_{i,j,k}^{back}\cdot n_{j,k}^{back}}{\sum_i^{mass}\sum_j^{tr(\mathcal{P}_{ev})}\sum_k^{X_E} N_{i,j,k}^{back}}\,. \tag{8}$$

The last contribution to the expectation was a term accounting for reflections from other decay modes, which are in particular necessary for the channel $D_s^+(\bar{K}^*)$ (see figure 6). They were taken directly from the simulation.

For the D_s^+ and Λ_c the average number of entries was only around 25. Therefore the number of entries per bin was no longer Gaussian distributed and a Poissonian statistic was taken instead. The fit was done maximising the likelihood:

$$\mathcal{L} = \sum_i^{mass}\sum_j^{tr(\mathcal{P}_{ev})}\sum_k^{X_E} \ln\left(\frac{\lambda_{i,j,k}^{N_{i,j,k}^{dat}}}{e^{\lambda_{i,j,k}}\cdot N_{i,j,k}^{dat}!}\right)\,. \tag{9}$$

Again, the equivalent R term was added to the likelihood.

6 Systematic uncertainties

Three major systematic error sources are considered for this analysis. The uncertainty in the Monte Carlo modelling of heavy quark production and decay can lead to changes in the predicted spectra of charm hadrons in $c\bar{c}$ and $b\bar{b}$ events. Problems in the simulation of the detector response on charm hadron events can affect the efficiency estimates. The fit method itself is also a potential source of systematic errors. The breakdown of the relative systematic errors on the measurements of $R_c P_{c\to D,\Lambda} BR$ and $R_b P_{b\to D,\Lambda} BR$ are given in tables 6 and 7, respectively.

The Monte Carlo modelling of heavy flavour production and decay affects the fit result in different ways. A change of the parameters leads to a different shape of the Monte Carlo signal spectra. Furthermore the selection efficiency and b-tagging is depending on the heavy flavour production and decay properties. Therefore it is necessary to correct for inadequate simulation settings. The corrections are done using JETSET to produce the required distribution and compare it to the one given in the full simulation before detector acceptance. The ratio of the two spectra is used as a weight to modify the Monte Carlo shape in equation 6. To estimate the systematic error the input value is changed within its error and the procedure is repeated.

The b lifetimes are corrected separately for B^+, B^0, Λ_b and B_s^0. Here the world averages $\tau(B^0) = 1.56 \pm 0.04$, $\tau(B^+) = 1.65 \pm 0.04$, $\tau(B_s^0) = 1.54 \pm 0.07$ and $\tau(\Lambda_b) = 1.22 \pm 0.05$ [13] are used to correct the simulation. For the systematic uncertainties belonging to this

Source	D^0	D^+	$D_s^+(\phi)$	$D_s^+(\bar{K}^*)$	Λ_c^+
$\tau(B^+, B^0, B_s^0, \Lambda_c)$ (see text)	∓ 0.7	∓ 0.6	∓ 0.9	∓ 1.0	∓ 0.8
$\langle X_E^c(D^*)\rangle = 0.510 \pm 0.009$	± 4.4	± 3.1	± 3.0	± 3.7	± 3.0
$\langle X_E^b(B)\rangle = 0.702 \pm 0.008$	± 0.2	± 0.3	± 0.2	± 0.3	± 0.1
$\epsilon_{b\to D} = 0.42 \pm 0.07$	∓ 0.6	∓ 0.7	∓ 0.5	∓ 0.6	∓ 0.3
$f(D^+, D_s^+, \Lambda_c)$ (see text)	∓ 0.3	∓ 0.4	∓ 0.8	∓ 2.1	∓ 0.3
$\tau(D^+, D^0, D_s^+, \Lambda_c)$ (see text)	± 0.7	± 0.7	± 1.0	± 2.5	± 1.7
$n_{g\to c\bar{c}} = (2.38 \pm 0.48)\%$	∓ 0.4	∓ 0.3	∓ 0.4	∓ 0.5	∓ 0.3
RICH(+dE/dx)	± 0.4	± 1.5	± 0.9	± 2.5	± 2.3
$\Delta L\, vs.\, X_E$	± 2.1	± 1.7	± 1.2	± 2.1	± 1.7
$\mathcal{P}(\chi^2)$	-	± 1.0	± 1.0	± 1.2	± 1.1
VD-hits	± 0.6	± 0.8	± 0.8	± 0.9	± 0.9
Tracking	∓ 2.0	∓ 3.0	∓ 3.0	∓ 3.0	∓ 3.0
b-tagging	± 1.0	± 0.9	± 0.8	± 1.4	± 1.3
MC-Statistics	± 1.7	± 1.9	± 6.9	± 10.9	± 9.5
$m(D, \Lambda)$ mean	± 0.3	± 0.2	± 0.4	± 1.4	± 1.4
$m(D, \Lambda)$ width	± 0.1	± 0.1	± 0.3	± 3.9	± 1.5
Reflections	∓ 0.1	∓ 0.7	∓ 0.6	∓ 4.8	∓ 0.8
Binning	± 0.6	± 1.9	± 4.4	± 5.2	± 3.2
Total	± 5.9	± 6.0	± 9.6	± 15.4	± 11.8

Table 6: *Relative systematic error on $R_c P_{c\to D,\Lambda} BR$ in %.*

source all the b lifetime distributions are regenerated at the edges of their errors and the fit is performed again. Similar to this procedure the c lifetimes are also corrected separately for D^+, D^0, Λ_c and D_s^+. Here the values $\tau(D^0) = 0.415 \pm 0.004$, $\tau(D^+) = 1.057 \pm 0.015$, $\tau(D_s^+) = 0.467 \pm 0.017$ and $\tau(\Lambda_c) = 0.206 \pm 0.012$ from [9] are taken.

The separation between $b\bar{b}$ and $c\bar{c}$ events obtained from the impact parameter tag depends on the rate of D^+ and D^0 mesons in $c\bar{c}$ events. Therefore the rates of charm hadrons in the hemisphere opposite to the reconstructed D or Λ are fixed to the present averages $f(D^+) = 0.221 \pm 0.020$, $f(D_s^+) = 0.112 \pm 0.027$ and $f(c_{baryon}) = 0.084 \pm 0.022$ [23]. The D^0 rate is calculated form these numbers according to

$$f(D^0) = 1 - f(D^+) - f(D_s^+) - f(c_{baryon})\,. \tag{10}$$

A one sigma error variation on each fraction is included in the systematic error, leaving the D^0 fraction free to keep the sum constant.

To allow for the uncertainty of the mean $\langle X_E^c(D)\rangle$ and $\langle X_E^b(B)\rangle$ the procedure is quite similar. JETSET is used to generate the $\langle X_E\rangle$ distributions of all charm ground states according to $\langle X_E^c(D^*)\rangle = 0.510 \pm 0.005 \pm 0.008$, $\langle X_E^b(B)\rangle = 0.702 \pm 0.008$ [9]. The energy spectrum of D mesons in the B rest frame was measured by CLEO [14]. This $\langle X_E^b(D)\rangle$ spectrum includes the contributions from $B \to D\,X$ and $B \to D\bar{D}\,X$. It can be parameterised in terms of a Peterson function with $\epsilon_{b\to D} = 0.42 \pm 0.07$ [11].

The corrections are applied on all simulated charm ground state hadrons separately for $b\bar{b}$ and $c\bar{c}$ events. The resulting X_E distribution of the sum of all charm hadron

Source	D^0	D^+	$D_s^+(\phi)$	$D_s^+(\bar{K}^*)$	Λ_c^+
$\tau(B^+, B^0, B_s^0, \Lambda_b)$ (see text)	± 2.4	± 2.4	± 2.8	± 3.1	± 3.9
$\langle X_E^c(D^*)\rangle = 0.510 \pm 0.009$	∓ 1.1	∓ 1.1	∓ 0.3	∓ 0.6	∓ 1.2
$\langle X_E^b(B)\rangle = 0.702 \pm 0.008$	± 3.1	± 1.8	± 1.9	± 2.3	± 2.9
$\epsilon_{b\to D} = 0.42 \pm 0.07$	∓ 3.8	∓ 1.2	∓ 1.8	∓ 2.2	∓ 0.8
$f(D^+, D_s^+, \Lambda_c)$ (see text)	± 0.1	± 0.1	± 0.2	± 0.6	± 0.1
$\tau(D^+, D^0, D_s^+, \Lambda_c)$ (see text)	± 0.3	± 0.5	± 0.1	± 0.1	± 0.1
$n_{g\to c\bar{c}} = (2.38 \pm 0.48)\%$	∓ 0.3	∓ 0.2	∓ 0.2	∓ 0.2	∓ 0.3
RICH(+dE/dx)	± 0.4	± 1.5	± 0.9	± 2.5	± 2.3
$\Delta L\, vs.\, X_E$	± 2.1	± 1.7	± 1.2	± 2.1	± 1.7
$\mathcal{P}(\chi^2)$	-	± 1.0	± 1.0	± 1.2	± 1.1
VD-hits	± 0.6	± 0.8	± 0.8	± 0.9	± 0.9
Tracking	∓ 2.0	∓ 3.0	∓ 3.0	∓ 3.0	∓ 3.0
b-tagging	∓ 1.3	∓ 1.0	∓ 1.0	∓ 1.3	∓ 2.0
MC-Statistics	± 2.0	± 2.8	± 3.3	± 5.0	± 4.1
$m(D, \Lambda)$ mean	± 0.1	± 0.1	± 0.8	± 1.9	± 1.6
$m(D, \Lambda)$ width	± 0.1	± 0.2	± 0.5	± 2.6	± 1.1
Reflections	∓ 0.1	∓ 0.5	∓ 0.5	∓ 2.0	∓ 0.9
Binning	± 0.5	± 2.1	± 2.0	± 2.3	± 3.5
Total	± 6.8	± 6.4	± 6.7	± 9.4	± 9.1

Table 7: *Relative systematic error on* $R_b P_{b\to D,\Lambda} BR$ *in %.*

ground states in $c\bar{c}$ events is found to be in agreement with the corresponding average of $\langle X_E^c(D^0, D^+)\rangle = 0.484 \pm 0.008$ [9]. Here the effect of gluon splitting is taken into account. The systematic uncertainties are calculated separately for $\langle X_E^c(D)\rangle$, $\langle X_E^b(B)\rangle$ and $\epsilon_{b\to D}$.

To account for gluon splitting into $c\bar{c}$ quark pairs, the $g \to c\bar{c}$ component is subtracted from the measured charm hadron spectra. Here the Monte Carlo prediction is scaled to reproduce the average value $n_{g\to c\bar{c}} = (2.38 \pm 0.48)\%$ [15]. The systematic uncertainty is obtained by varying the rate within the error.

A good description of the detector acceptance is needed to extract the efficiency correction from the Monte Carlo. Therefore a careful tuning to correct for residual problems in the Monte Carlo description is done in all stages of the analysis. The decay channel $D^{*+} \to (K^-\pi^+)\pi^+$ is chosen to study the systematic errors due to the selection of charm hadrons. Since this decay channel is also used for analysis, none of the cuts discussed in the following have been performed on it. The D^{*+} sample is analysed in a window around the mass difference between the D^0 and the remaining slow π^+. For a cut applied to reconstruct a given decay channel, the inefficiencies $\bar{\epsilon}$ are computed in data from a fit to the corresponding D^{*+} mass spectrum of rejected events and compared to the Monte Carlo result. For a residual discrepancy between these inefficiencies a factor

$$f_{corr} = \frac{1 - \bar{\epsilon}_{data}}{1 - \bar{\epsilon}_{MC}} \tag{11}$$

is introduced to correct the Monte Carlo description of the efficiency. The relative statistical uncertainty of the correction factor is taken as the systematic error.

The combined RICH and dE/dx tagging used to reconstruct the different charm hadrons is tested using the kaon from the D^0 in the D^{*+} channel. For each decay mode the same cuts are applied to the D^{*+} sample. To reconstruct the $D_s^+(\bar{K}^*)$ channel both kaons are required to be tagged. A very tight $\Lambda^0 \to p\pi^-$ sample is used to test the proton identification for the Λ_c^+ channel. Only protons from Λ^0 with a momentum above the cut applied to the Λ_c^+ sample are used for this study.

The cut on the vertex fit χ^2 probability $\mathcal{P}(\chi^2)$ is also tested using the D^* sample. Fitting all three products of the $D^{*+} \to (K^-\pi^+)\pi^+$ decay into one common vertex is a good approximation for a three body decay vertex, since the pion from the D^{*+} decay has a small p_t w.r.t. the D^0.

The energy dependent cuts on the measured decay length ΔL of the charm hadron can be tested using the D^0 from the D^{*+} sample. The correction for the D^+ channel is computed scaling the measured D^0 decay length by the lifetime ratio of $\tau(D^+)/\tau(D^0)$.

The requirement of all candidate tracks to have at least one VD hit associated is again tested with the D^* decay, leaving out the slow pion in case of the D^0. A summary of all correction factors applied to the fitted rates can be found in table 8.

It has been checked that the product of the efficiency correction factors obtained is in good agreement with the overall correction for the VD hit, $\mathcal{P}(\chi^2)$, RICH($+dE/dx$) and $\Delta L\, vs.\, X_E$ cuts.

The charged track reconstruction efficiency is another possible source of systematic errors. In reference [16] the tracking efficiency in DELPHI has been determined to be 0.989 ± 0.001. The difference between data and Monte Carlo in the region of the TPC ϕ boundaries was estimated to be 0.2%. Following reference [16] the 1% inefficiency of the track reconstruction is used as the systematic error of the track reconstruction.

The systematic effect due to the efficiency of the b-tagging was studied in reference [17] using a tuning determined independently on data and Monte Carlo. A residual difference in the b efficiency of 3 % per jet between data and Monte Carlo was found. The corrections to the physics parameters in the Monte Carlo mentioned above accounts for most of the difference. Therefore only 30 % of the difference is taken for the systematic error.

Particle	RICH($+dE/dx$)	$\Delta L\, vs.\, X_E$	$\mathcal{P}(\chi^2)$	VD-hits
D^0	0.9989±0.0042	1.0048±0.0206	–	1.0067±0.0064
D^+	0.9528±0.0148	1.0137±0.0175	0.9579±0.0097	1.0017±0.0084
$D_s^+(\phi)$	1.0054±0.0093	1.0113±0.0117	0.9563±0.0099	1.0017±0.0084
$D_s^+(K^*)$	0.9875±0.0250	1.0109±0.0206	0.9519±0.0122	1.0110±0.0088
Λ_c^+	0.9339±0.0226	1.0096±0.0174	0.9501±0.0114	1.0110±0.0088

Table 8: *Correction factors applied due to cut inefficiency discrepancies*

The systematic error due to the statistical error of the Monte Carlo is given in tables 6 and 7. For the D^0 and D^+ this error is included directly in the χ^2 definition. For the binned likelihood fit to the D_s^+ and Λ_c^+ spectra the error due to the limited number of Monte Carlo events is evaluated using a statistical method. The distribution of 3000 fit results using random Monte Carlo sets reflects the total statistical error while the error obtained from the fits only includes the statistical error of the data set itself. Hence

the quadratic difference of both errors is taken as the contribution of the Monte Carlo statistical error.

The shape of the mass signal is a possible source of systematic errors. Therefore the variation of the mean and the width of the mass signal shape is included in the systematic error table.

The rate of reflections affect the background shape under the signal. Especially for the $D_s^+(\bar{K}^*)$ channel changes in the rates of the reflections lead to variations in the fit result. The systematic error assigned corresponds to a 30% variation of the reflection rates.

Finally the effect of the binning in the three dimensional fit of the charm counting analysis is studied by varying the number of bins in each dimension by $\pm$ 1 bin. All systematic errors for the different decay channels are summed up quadratically to obtain the total systematic errors given in tables 6 and 7. In the following calculations the systematic errors due to the Monte Carlo modelling and the detector acceptance are assumed to be fully correlated between the different channels.

7 Fit results

From a three dimensional fit of the charm hadron *mass* spectra, the scaled energy X_E and the impact parameter information $tr(\mathcal{P}_{ev})$ the products $R_c P_{c\to D,\Lambda}\, BR$ and $R_b P_{b\to D,\Lambda}\, BR$ were measured. The results using the DELPHI data taken in 1992-1995 are shown in table 9. The first error denotes the statistical uncertainty, the second error corresponds to the systematic error discussed above. The numbers include the efficiency corrections given in table 8. The D_s^+ rates are corrected for the branching ratio $\phi \to K^-K^+ = (49.1 \pm 0.8)\%$ [18] and $\bar{K}^*(892) \to K^-\pi^+ = 2/3$. The correlation between the measured production rates for $c\bar{c}$ and $b\bar{b}$ events is given in the last column.

Mode	$R_c P_{c\to D,\Lambda}\, BR \times 10^3$	$R_b P_{b\to D,\Lambda}\, BR \times 10^3$	*correlation* %
$D^0 \to K^-\pi^+$	$3.598 \pm 0.101 \pm 0.212$	$5.042 \pm 0.164 \pm 0.343$	-46
$D^+ \to K^-\pi^+\pi^+$	$3.494 \pm 0.116 \pm 0.210$	$4.525 \pm 0.204 \pm 0.290$	-38
$D_s^+ \to \phi(1020)\pi^+$	$0.765 \pm 0.069 \pm 0.073$	$1.259 \pm 0.100 \pm 0.084$	-30
$D_s^+ \to \bar{K}^*(892)K^+$	$0.624 \pm 0.122 \pm 0.096$	$1.179 \pm 0.159 \pm 0.111$	-30
$\Lambda_c^+ \to pK^-\pi^+$	$0.743 \pm 0.155 \pm 0.088$	$0.962 \pm 0.187 \pm 0.088$	-30

Table 9: *Results on $R_{c(b)}P_{c(b)\to D,\Lambda}BR$ from the combined fit to the data. The first error is statistical, the second belongs to systematics.*

Based on these numbers, the product of $R_{c(b)}$ and the production probability $P_{c(b)\to D,\Lambda}$ can be calculated for the charm counting using the branching ratios given in table 10 from reference [18].

No precise measurement for the branching ratio $D_s^+ \to \bar{K}^*(892)K^+$ has been done so far. Therefore the ratio $BR(D_s^+ \to \bar{K}^*(892)K^+)/BR(D_s^+ \to \phi(1020)\pi^+)$ is used. The results for both decay modes are compared in table 11. The third error given in addition to the statistical and systematic error corresponds to the uncertainty of the branching ratios. The average given in the table is computed taking all correlations into account. The statistical correlation of the averages for $c\bar{c}$ and $b\bar{b}$ events is -30%.

A summary of the measured rates of D^0, D^+, D_s^+ and Λ_c^+ from $c\bar{c}$ and $b\bar{b}$ events is given in table 12.

Mode	branching ratio
$D^0 \to K^-\pi^+$	0.0385 ± 0.0009
$D^+ \to K^-\pi^+\pi^+$	0.091 ± 0.006
$D_s^+ \to \phi(1020)\pi^+$	0.035 ± 0.009
$\frac{BR(D_s^+ \to \bar{K}^* K^+)}{BR(D_s^+ \to \phi\pi^+)}$	0.95 ± 0.10
$\Lambda_c^+ \to pK^-\pi^+$	0.050 ± 0.013

Table 10: *Branching ratios used for the charm fraction measurements.*

Mode	$R_c P_{c\to D_s^+} \times 10^2$	$R_b P_{b\to D_s^+} \times 10^2$
$D_s^+ \to \phi(1020)\pi^+$	$2.189 \pm 0.198 \pm 0.211 \pm 0.562$	$3.596 \pm 0.286 \pm 0.241 \pm 0.925$
$D_s^+ \to \bar{K}^*(892)K^+$	$1.877 \pm 0.366 \pm 0.288 \pm 0.521$	$3.545 \pm 0.478 \pm 0.334 \pm 0.985$
average	$2.109 \pm 0.175 \pm 0.188 \pm 0.537$	$3.586 \pm 0.245 \pm 0.237 \pm 0.914$

Table 11: *Results on $R_{c(b)} P_{c(b)\to D_s^+}$ including correlations*

Mode	$R_c P_{c\to D,\Lambda} \times 10^2$	$R_b P_{b\to D,\Lambda} \times 10^2$
D^0	$9.346 \pm 0.261 \pm 0.547 \pm 0.219$	$13.095 \pm 0.427 \pm 0.889 \pm 0.306$
D^+	$3.839 \pm 0.128 \pm 0.229 \pm 0.253$	$4.973 \pm 0.224 \pm 0.320 \pm 0.328$
D_s^+	$2.109 \pm 0.175 \pm 0.188 \pm 0.537$	$3.586 \pm 0.245 \pm 0.237 \pm 0.914$
Λ_c^+	$1.487 \pm 0.311 \pm 0.175 \pm 0.387$	$1.924 \pm 0.374 \pm 0.175 \pm 0.500$

Table 12: *Contributions to charm counting in $c\bar{c}$ and $b\bar{b}$ events. The first error is statistical, the second belongs to systematics and the third is due to the error on the branching ratio.*

8 Measurements of R_c

For this measurement, R_c is given by the sum of all weakly decaying charm hadron rates. The results presented in table 12 do not include strange charm baryon production. Following the argumentation in reference [2] and [9] the rates of these baryons are estimated from the light quark sector. The ratio Ξ^-/Λ is measured to be $(6.9 \pm 0.4)\%$ and the Ω^-/Λ ratio is $(0.44 \pm 0.08)\%$ [18]. Assuming equal production of Ξ^- and Ξ^0 one expects about 14% of strange charm baryon production relative to the Λ_c rate. The error assigned to

this rate is 5%. Therefore a contribution of 0.00208 ± 0.00074 for Ξ_c and Ω_c is added to the measured rates. Taking correlated systematic errors into account one obtains:

$$R_c = 0.1699 \pm 0.0049(stat) \pm 0.0096(syst) \pm 0.0078(Br)\,. \tag{12}$$

A full set of parameters as used by the LEP heavy flavour working group is given in table 13 together with the correlation matrix.

parameter	value	error	R_c	$f(D^+)$	$f(D_s^+)$	$f(c_{bary})$
R_c	0.1699	0.0133	1.00	-.30	0.32	0.37
$f(D^+)$	0.2260	0.0186	-.30	1.00	-.37	-.39
$f(D_s^+)$	0.1242	0.0307	0.32	-.37	1.00	-.23
$f(c_{bary})$	0.0997	0.0320	0.37	-.39	-.23	1.00

Table 13: *Full set of parameters as used by the LEP heavy flavour working group with correlation matrix.*

9 Charm counting in *b* decays

To extract from table 12 the number of charm quarks per b decay one has to sum up all weakly decaying charm states. This includes charmonia $c\bar{c}$ states which count twice and strange charm baryons.

The $b \to charmonia$ rates given in table 14 have been measured by DELPHI [19]. From these numbers one can estimate the total rate of charmonia production in b decays assuming a ratio of $\eta_c : J/\psi : \chi_{c1} : \psi' = 0.57 : 1. : 0.27 : 0.31$ [20] for the different states. J/ψ and χ_{c1} production due to radiative charmonia decays are estimated using $BR(\psi' \to \chi_{c1}\gamma) = (8.7 \pm 0.8)\%$, $BR(\psi' \to J/\psi X) = (54.2 \pm 3.0)\%$ and $BR(\chi_{c1} \to J/\psi\gamma) = (27.3 \pm 1.6)\%$ [18]. One obtains $f(b \to charmonia\, X) = 0.0200 \pm 0.0024 \pm 0.0060$ for the total rate. The first error reflects the error of the measurements and of the branching ratios, the second error corresponds to a 30% uncertainty assigned to the theoretical prediction of reference [20].

The rates $R_b P_{b\to D,\Lambda}$ given in table 12 are translated into $P_{b\to D,\Lambda}$ using the present average $R_b = 0.2170 \pm 0.0009$ [23]. The summary of measured contributions to the charm counting in $b\bar{b}$ events is shown in table 15.

The production rate of $f(b \to \Xi_c X)$ is not measured. To estimate its value we follow the argumentation from reference [21]. CLEO [22] has measured the rates of $f(\bar{B} \to \Xi_c^+) = 0.008 \pm 0.005$ and $f(\bar{B} \to \Xi_c^0) = 0.012 \pm 0.009$. The PDG values[18] for rates of b hadrons in Z events are $(39.7^{+1.8}_{-2.2})\%$ for B^0 and B^+, $(10.5^{+1.8}_{-1.7})\%$ for B_s^0 and $(10.1^{+3.9}_{-3.1})\%$ for b-baryons. One obtains a rate of 0.023 ± 0.013 Ξ_c baryons from B mesons. Using JETSET one estimates $f(b_{baryon} \to \Xi_c X) = 0.22 \pm 0.11$, which adds 0.022 ± 0.013 to the total Ξ_c rate. Adding the Ξ_c baryon contribution 0.045 ± 0.018 to the measured rates from table 15 one gets:

$$n_c = 1.172 \pm 0.031(stat) \pm 0.070(syst) \pm 0.052(Br)\,. \tag{13}$$

Mode	$P_{b\to X_c} \times 10^2$
J/ψ	$1.12 \pm 0.12(stat) \pm 0.10(sys)$
ψ'	$0.48 \pm 0.22(stat) \pm 0.10(sys)$
χ_{c1}	$1.4 \pm 0.6(stat)^{+0.4}_{-0.2}(sys)$

Table 14: *DELPHI published charmonia rates from b decays.*

Mode	$P_{b\to X_c} \times 10^2$
D^0	$60.35 \pm 1.96 \pm 4.09 \pm 1.41$
D^+	$22.92 \pm 1.03 \pm 1.47 \pm 1.51$
D_s^+	$16.52 \pm 1.13 \pm 1.08 \pm 4.21$
Λ_c^+	$8.86 \pm 1.72 \pm 0.81 \pm 2.30$
$charmonia(*2)$	$4.00 \pm 0.48 \pm 1.20$
total measured	$112.65 \pm 3.02 \pm 6.75 \pm 5.23$

Table 15: *Contributions to charm counting in $b\bar{b}$ events. The first error is statistical, the second belongs to systematics and the third is due to the branching ratios.*

10 Conclusions

The results on R_c and n_c presented in this note are based on the DELPHI data taken from 1992 to 1995. R_c was measured from the overall charm counting:

$$R_c = 0.1699 \pm 0.0049(stat) \pm 0.0096(syst) \pm 0.0078(Br)\,. \tag{14}$$

The result on R_c improves the precision compared to previous DELPHI results [4] using exclusive D. Good agreement is found with other LEP results [23] and the prediction of the Standard Model.

A comparison of the measured result on n_c:

$$n_c = 1.172 \pm 0.031(stat) \pm 0.070(syst) \pm 0.052(Br)\,,$$

together with the DELPHI results on semileptonic b branching ratio B_{SL} [24], with the theoretical expectation from reference [25] is shown in figure 19. The measured n_c value also agrees well with the other DELPHI result $n_c = 1.147 \pm 0.041$[26] using an indirect method to extract the charmless and double charm contribution from the b tagging spectrum. The results on the individual production rates in $b\bar{b}$ events agree well with numbers reported by OPAL [2] and ALEPH [21]. Only the different assumptions on strange charm baryon production give rise to larger differences between the measurements and to the result reported by CLEO [22].

11 Acknowledgements

We thank the SL division of CERN for the excellent performance of the LEP collider and their careful work on the beam energy determination. We are also grateful to the

technical and engineering staffs in our laboratories and to our funding agencies for their continuing support.

References

[1] G.Altarelli and S.Petrarca, Phys. Lett. **B 261** (1991) 303;
I.Bigi et al., Phys. Lett. **B 323** (1994) 408.

[2] G.Alexander et al., OPAL Collaboration, Z. Phys. **C 72** (1996) 1.

[3] K. Ackerstaff et al., OPAL Collaboration, Eur. Phys. J. **C 1** (1998) 439;
R.Barate et al., ALEPH Collaboration, CERN/EP/98-035, Euro. Phys. J. **C** to be published.

[4] D.Bloch et al., DELPHI Collaboration, *Summary of R_c Measurements in DELPHI*, ICHEP'96 Ref. pa01-60, DELPHI 96-110 CONF 37, Geneva 1996.

[5] P.Abreu et al., DELPHI Collaboration, Nucl. Inst. and Meth. **A 378** (1996) 57.

[6] T.Sjöstrand, Comp. Phys. Comm. **39** (1986) 347 ;
T.Sjöstrand and M.Bengtsson, Comp. Phys. Comm. **43** (1987) 367.

[7] P.Abreu et al., DELPHI Collaboration, Zeit. Phys. **C 71** (1996) 11.

[8] C.Peterson, D.Schlatter, J.Schmitt and P.Zerwas, Phys. Rev. **D27** (1983) 105.

[9] The LEP Electroweak Working Group, *Presentation of LEP Electroweak Heavy Flavour Results for the Summer 1996 Conferences*, LEPHF/96-01, DELPHI 96-67 PHYS 627, Geneva 1996.

[10] E.Schyns, *NEWTAG - π, K, p Tagging for Delphi RICHes*, DELPHI 96-103 RICH 89, Geneva 1996.

[11] The LEP Electroweak Working Group, *A consistent treatment of systematic Errors for LEP electroweak Heavy Flavour Analyses*, LEPHF/94-01, DELPHI 94-23 PHYS 357.

[12] G. Borisov and C. Mariotti, Nucl. Instr. & Meth. **A372** (1996) 181.

[13] L. Di Ciaccio, private communication, to be published in the PDG 98.

[14] D.Bortoletto et al., CLEO Collaboration, Phys. Rev. **D 45** (1992) 21.

[15] R. Akers et al., OPAL Collaboration, Phys. Lett. **B 353** (1995) 595.

[16] P. Abreu et al., DELPHI Collaboration, Phys. Lett. **B 425** (1998) 399.

[17] G.J.Barker et al., DELPHI Collaboration, *A precise measurement of the partial decay width ratio $R_b^0 = \Gamma_{b\bar{b}}/\Gamma_{had}$*, ICHEP'97 #123, DELPHI 98-123 CONF 184, Geneva 1998.

[18] Review of Particle Physics, Euro. Phys. J. C3 (1998), 1.

[19] P.Abreu et al., DELPHI Collaboration, Phys. Lett. **B 341** (1994) 109.

[20] J.H.Kühn, S.Nussinov, R.Rüdel, Z. Phys. **C 5** (1980) 117.

[21] D.Buskulic et al., ALEPH Collaboration, Phys. Lett. **B 388** (1996) 648.

[22] L.Gibbons et al., CLEO Collaboration, Phys. Rev. **D 56** (1997) 3783.

[23] The LEP Electroweak Working Group, *A Combination of Preliminary Electroweak Measurements and Constraints on the Standard Model*, CERN-PPE/97-154, Geneva 1997.

[24] M.Calvi, *Measurement of the semileptonic b branching ratios and $\bar{\chi}_b$ from inclusive leptons in Z decays*, ICHEP'98 #129, DELPHI 98-122 CONF 183, Geneva 1998.

[25] M.Neubert and C.T.Sachrajda, Nucl. Phys. **B 483** (1997) 339.

[26] P.Abreu et al., DELPHI Collaboration, *Measurement of the inclusive charmless and double-charm B branching ratios*, CERN-PPE/98-07, Geneva 1998.

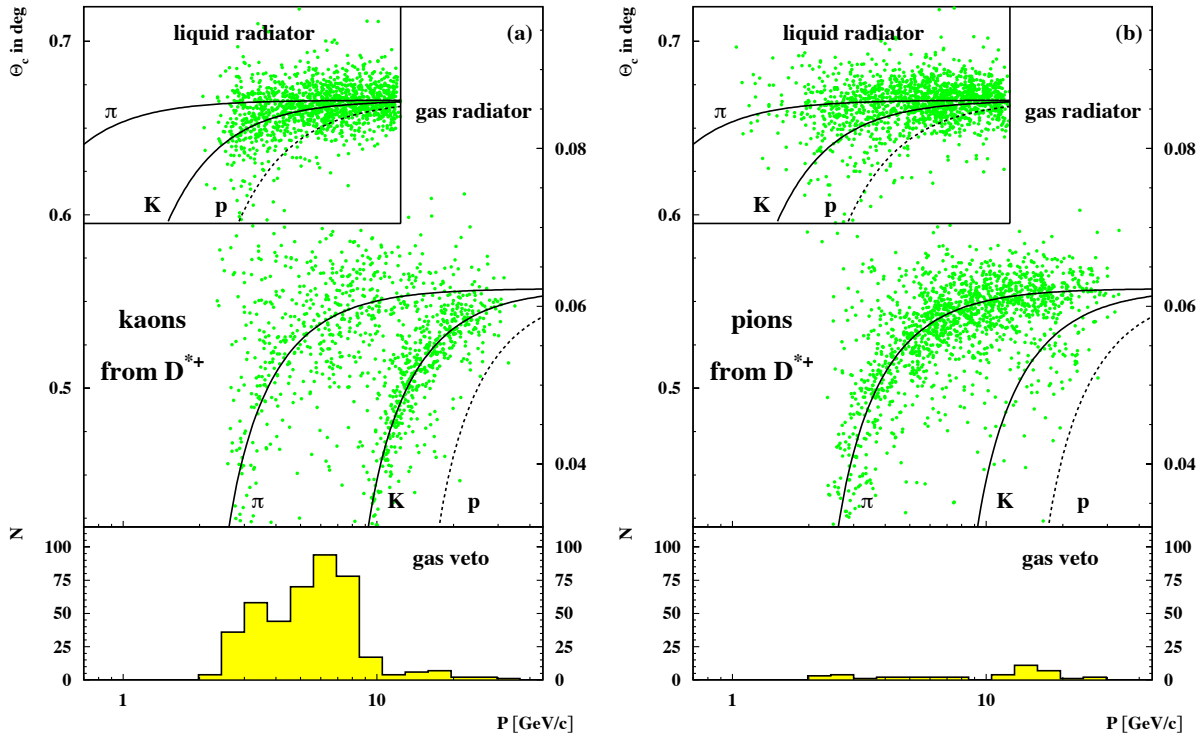

Figure 1: *The response of the DELPHI RICH gas and liquid radiators for (left) kaons and (right) pions from D^{*+} decay candidates. Shown is the measured Cherenkov angle in the gas radiator and the liquid radiator (insert), as well as the veto counts (lower part) as a function of the track momentum. The bands indicate the predicted Cherenkov angle for pions, kaons and proton.*

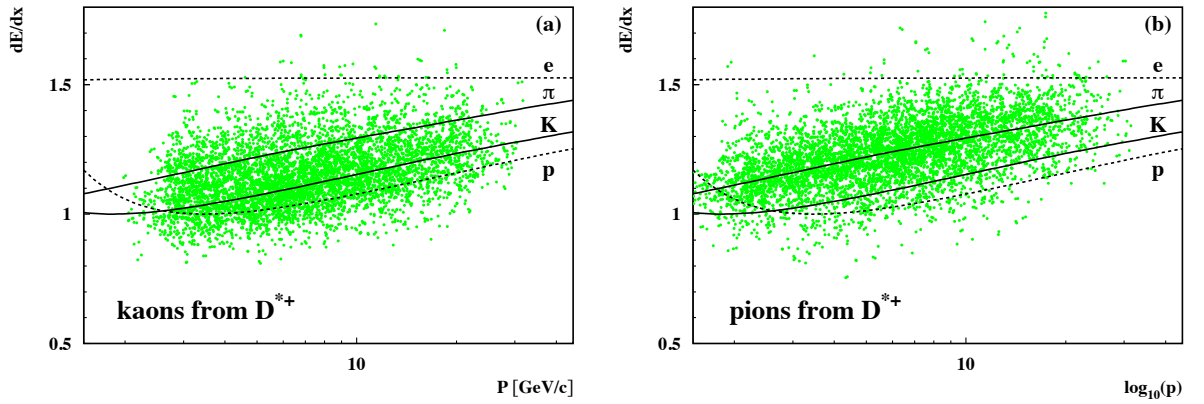

Figure 2: *The measured specific energy loss of (left) kaons and (right) pions from D^{*+} as a function of the track momentum. The expectation for kaons and pions is shown as lines.*

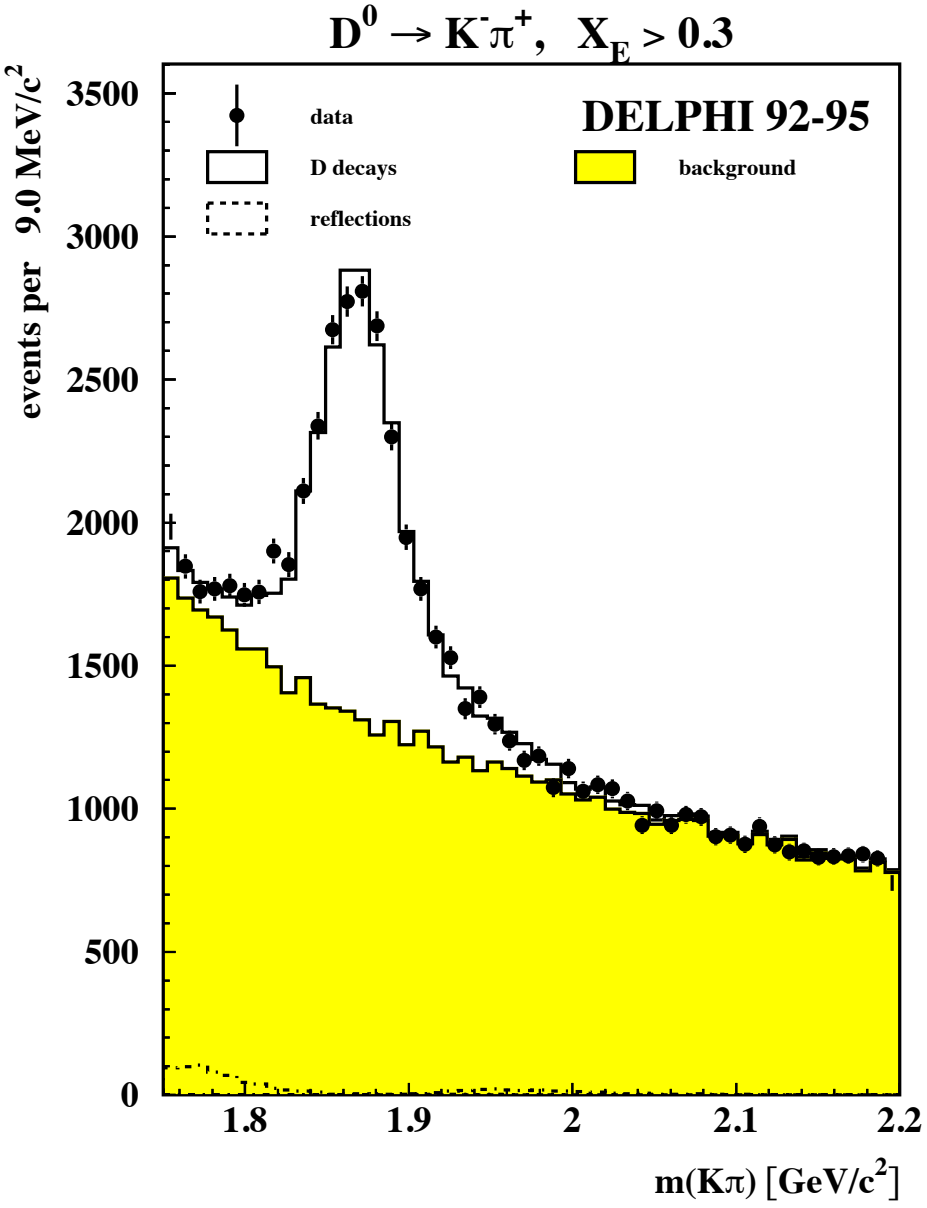

Figure 3: *Invariant $K\pi$ mass spectrum showing the D^0 mass signal. Contributions from reflections are shown as a dotted line.*

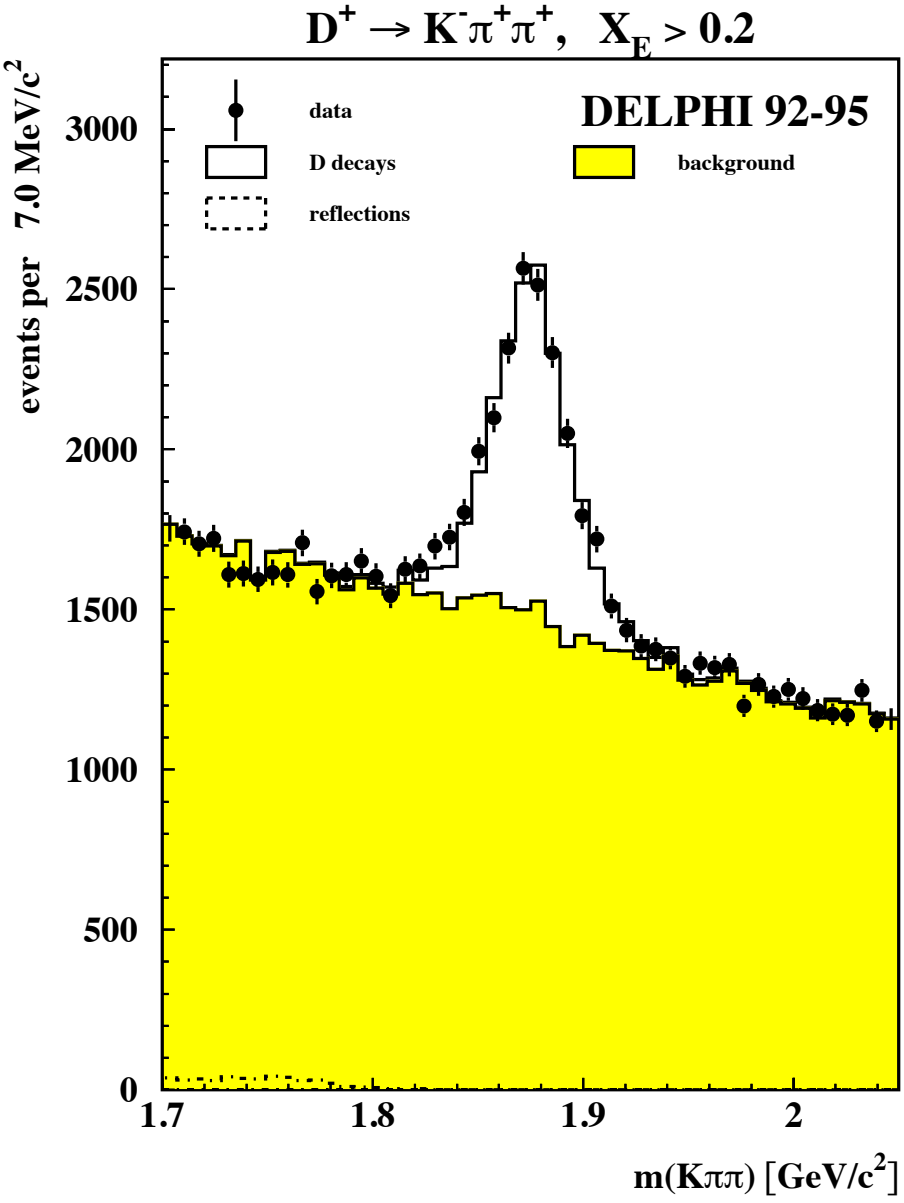

Figure 4: *Invariant $K\pi\pi$ mass spectrum showing the D^+ mass signal.*

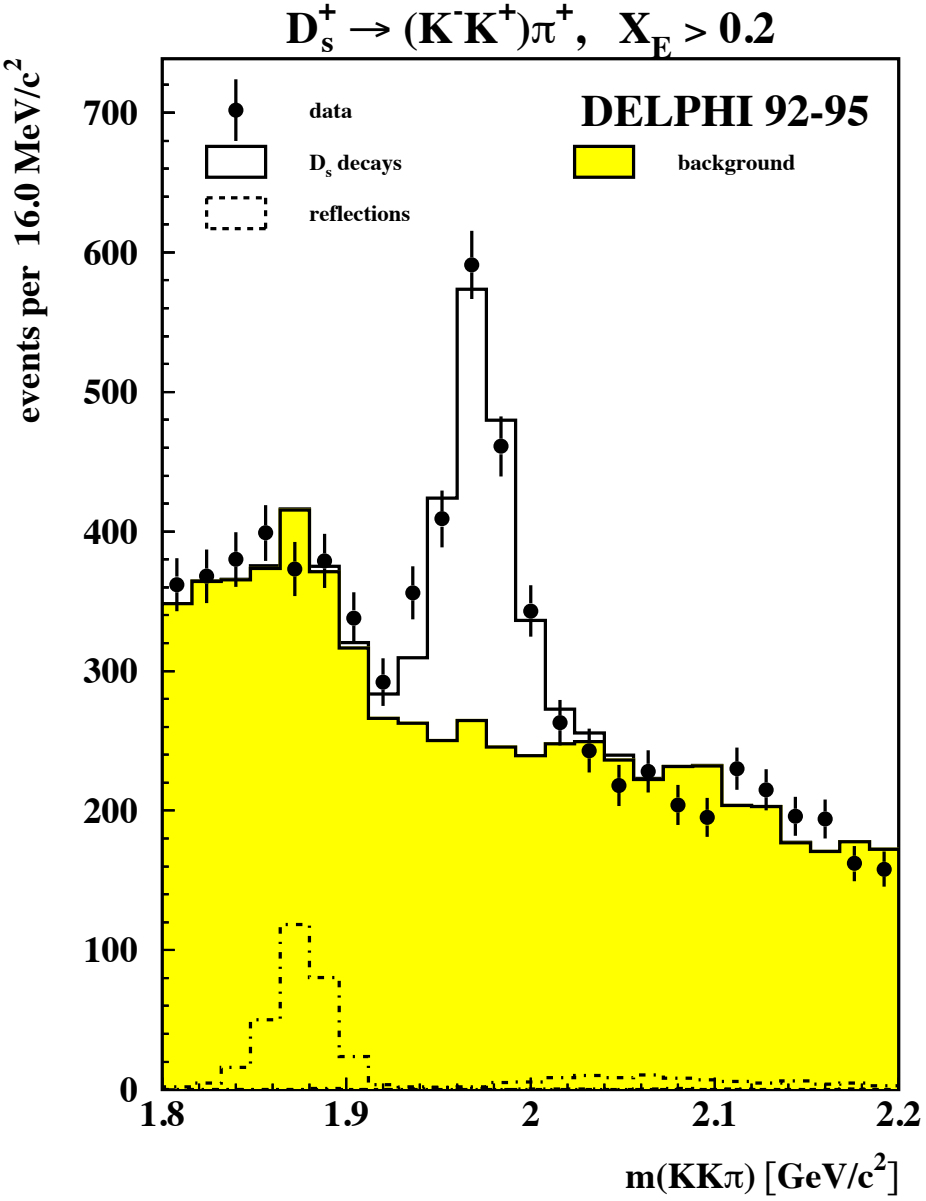

Figure 5: *Invariant mass spectrum for the decay* $D_s^+ \to \phi(1020)\pi^+$. *The contributions from* D^{*+} *decays are described in the tex.*

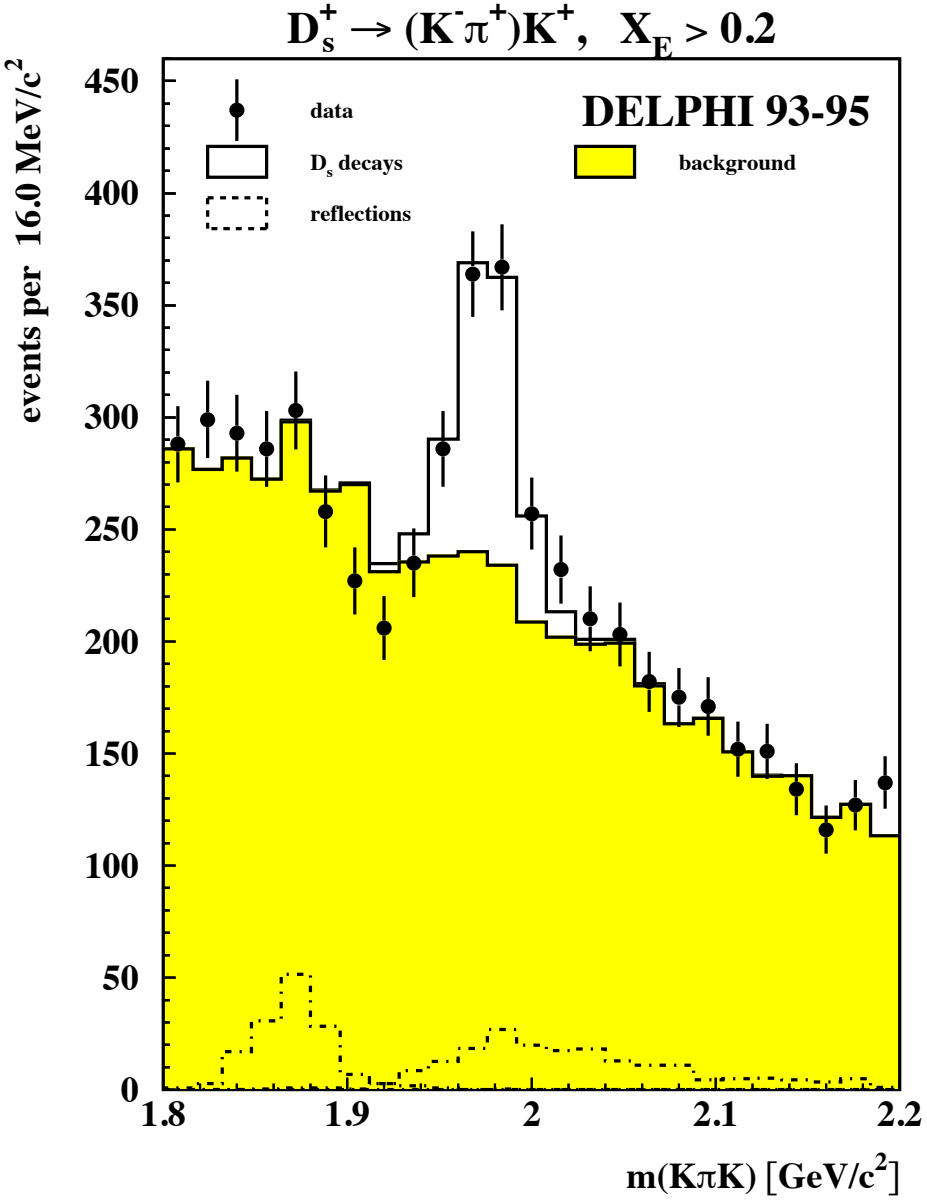

Figure 6: *Invariant mass spectrum for the decay* $D_s^+ \to \bar{K}^*(892)K^+$. *The contributions from* D^{*+} *decays are described in the tex.*

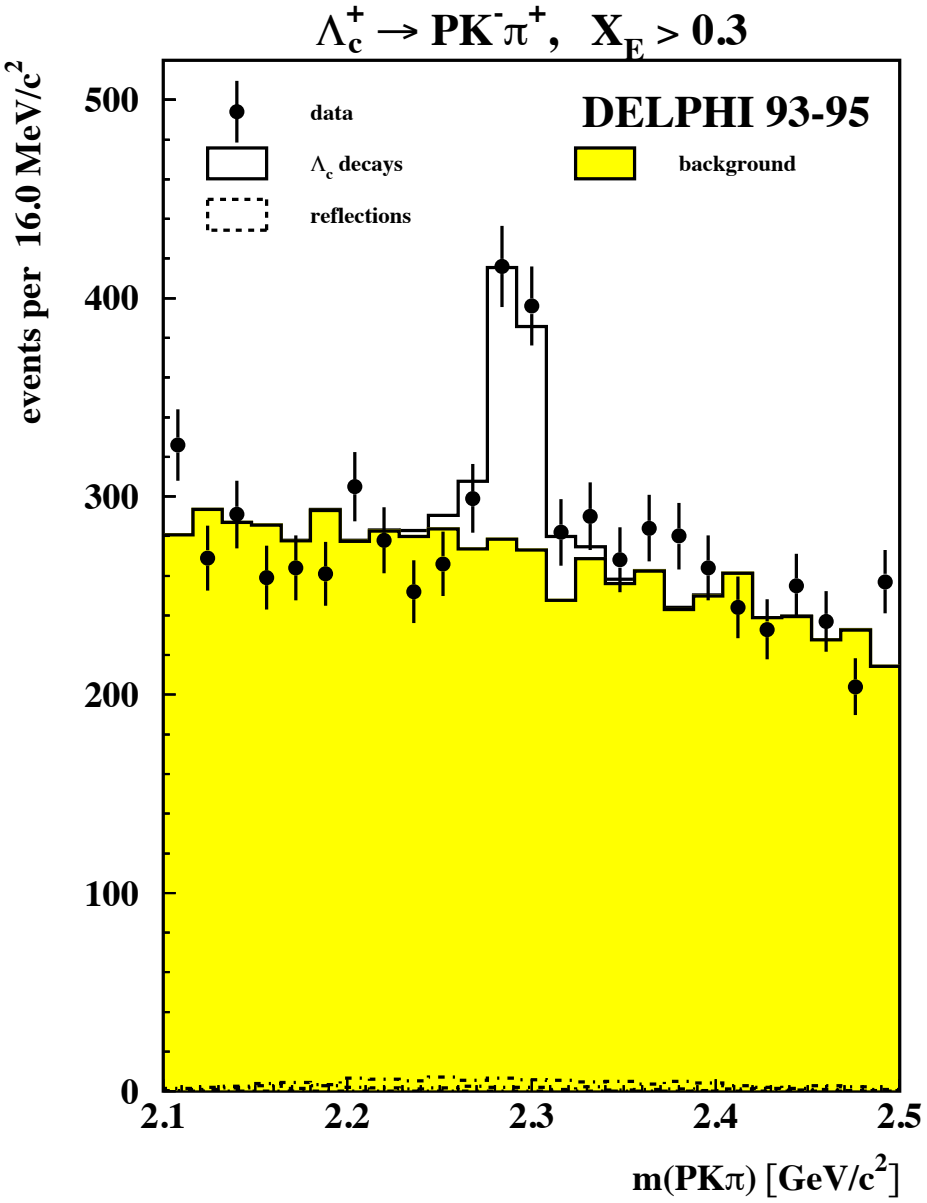

Figure 7: *Invariant mass spectrum for the decay* $\Lambda_c^+ \to pK^-\pi^+$.

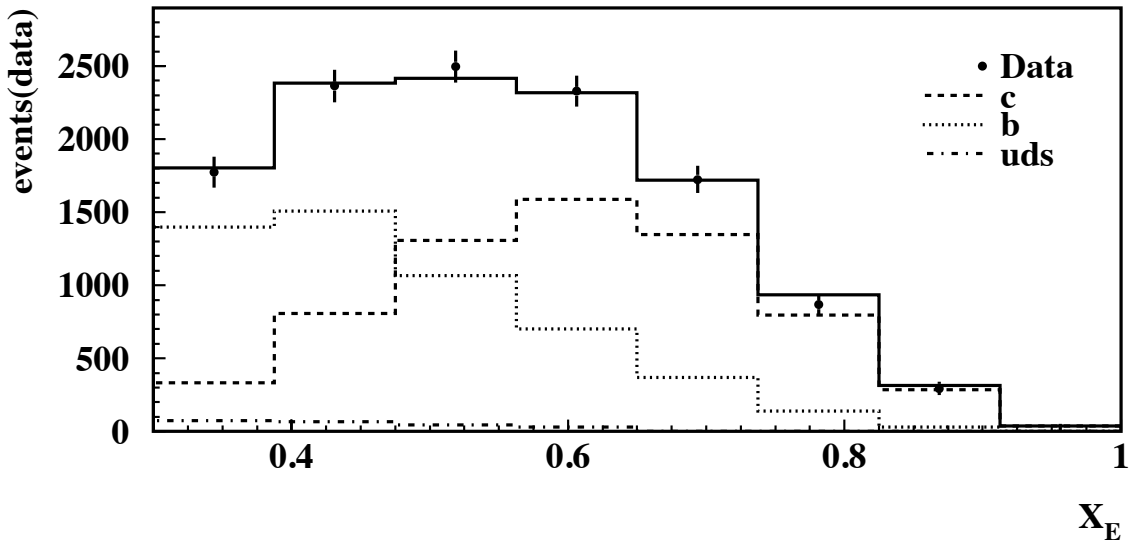

Figure 8: *Background subtracted X_E spectrum for the decay $D^0 \to K^-\pi^+$. No efficiency correction is applied. The reconstructed Monte Carlo spectra for $b\bar{b}$ and $c\bar{c}$ events is scaled in order to reproduce the fit results as described in the text.*

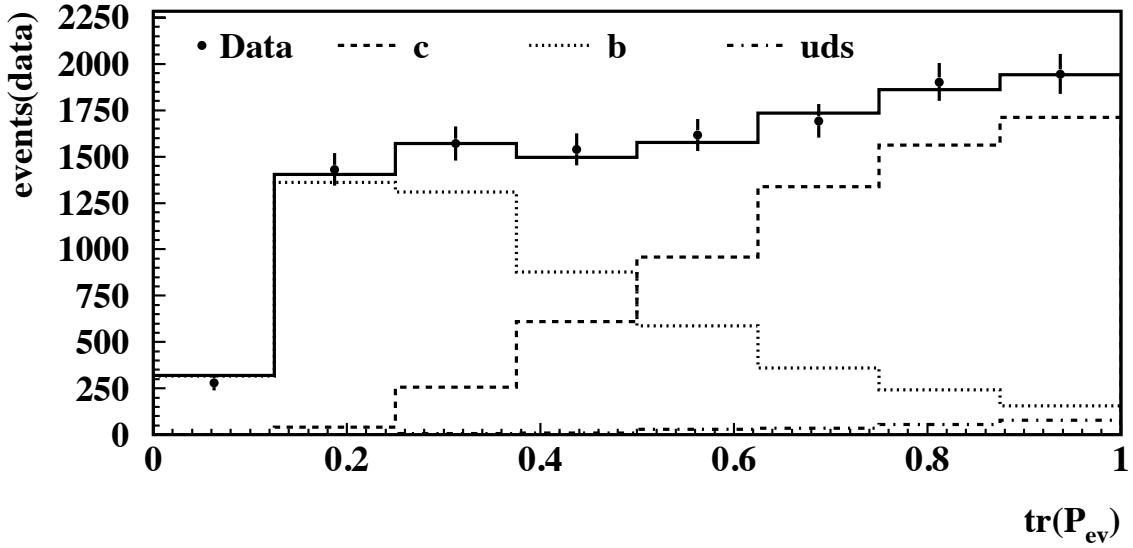

Figure 9: *Background subtracted $tr(\mathcal{P}_{ev})$ spectrum for the decay $D^0 \to K^-\pi^+$. No efficiency correction is applied. The reconstructed Monte Carlo spectra for $b\bar{b}$ and $c\bar{c}$ events is scaled in order to reproduce the fit results as described in the text.*

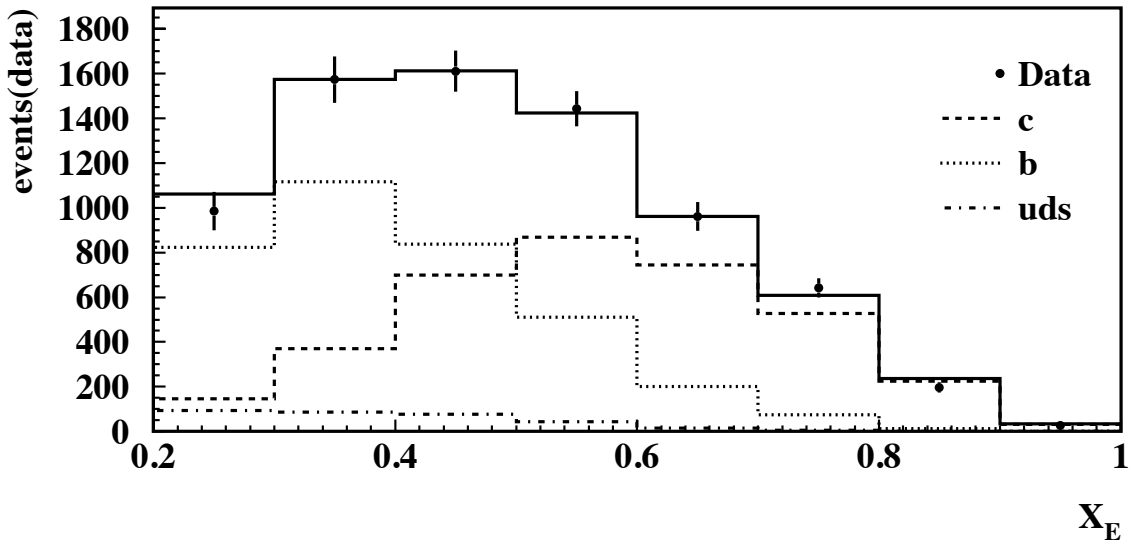

Figure 10: *Background subtracted X_E spectrum for the decay $D^+ \to K^-\pi^+\pi^+$. No efficiency correction is applied. The reconstructed Monte Carlo spectra for $b\bar{b}$ and $c\bar{c}$ events is scaled in order to reproduce the fit results as described in the text.*

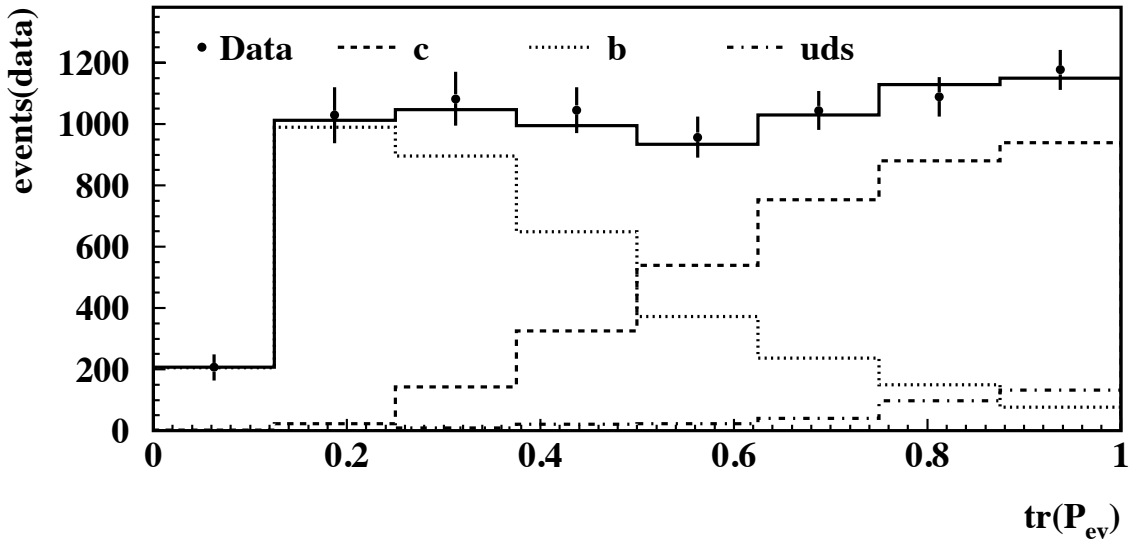

Figure 11: *Background subtracted $tr(\mathcal{P}_{ev})$ spectrum for the decay $D^+ \to K^-\pi^+\pi^+$. No efficiency correction is applied. The reconstructed Monte Carlo spectra for $b\bar{b}$ and $c\bar{c}$ events is scaled in order to reproduce the fit results as described in the text.*

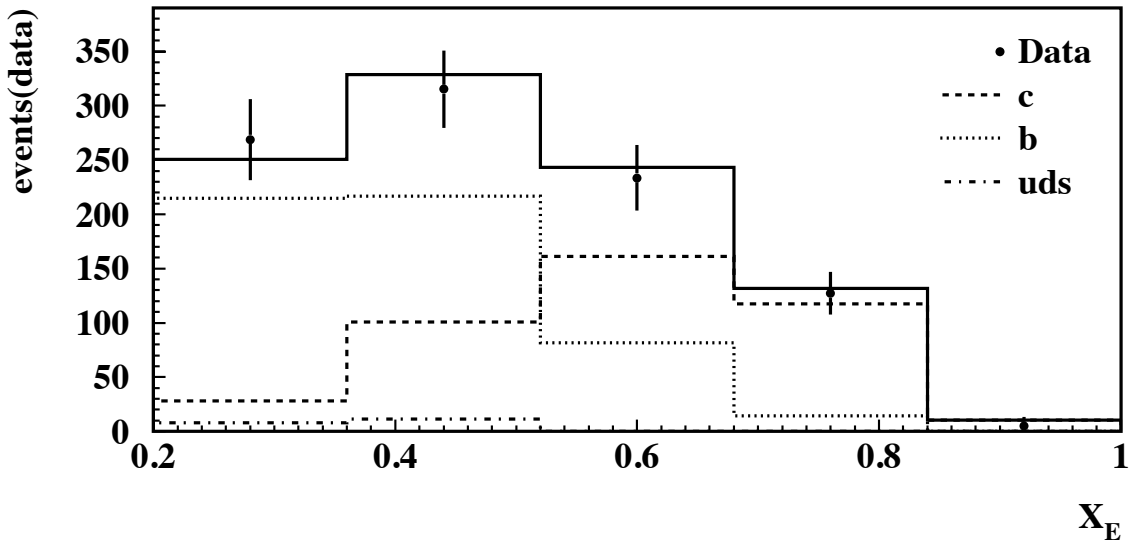

Figure 12: *Background subtracted X_E spectrum for the decay $D_s^+ \to \phi(1020)\pi^+$. No efficiency correction is applied. The reconstructed Monte Carlo spectra for $b\bar{b}$ and $c\bar{c}$ events is scaled in order to reproduce the fit results as described in the text.*

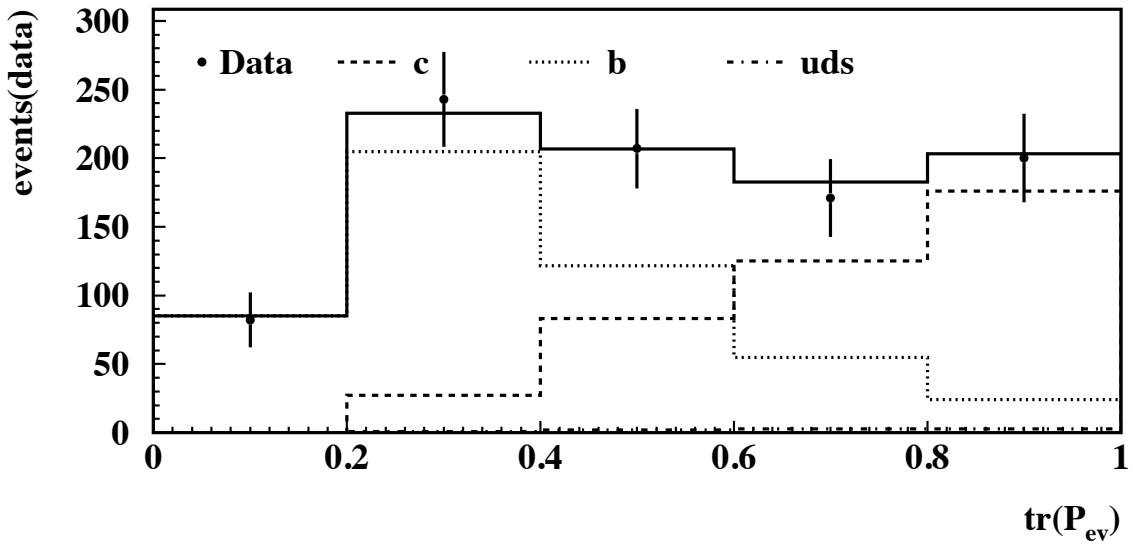

Figure 13: *Background subtracted $tr(\mathcal{P}_{ev})$ spectrum for the decay $D_s^+ \to \phi(1020)\pi^+$. No efficiency correction is applied. The reconstructed Monte Carlo spectra for $b\bar{b}$ and $c\bar{c}$ events is scaled in order to reproduce the fit results as described in the text.*

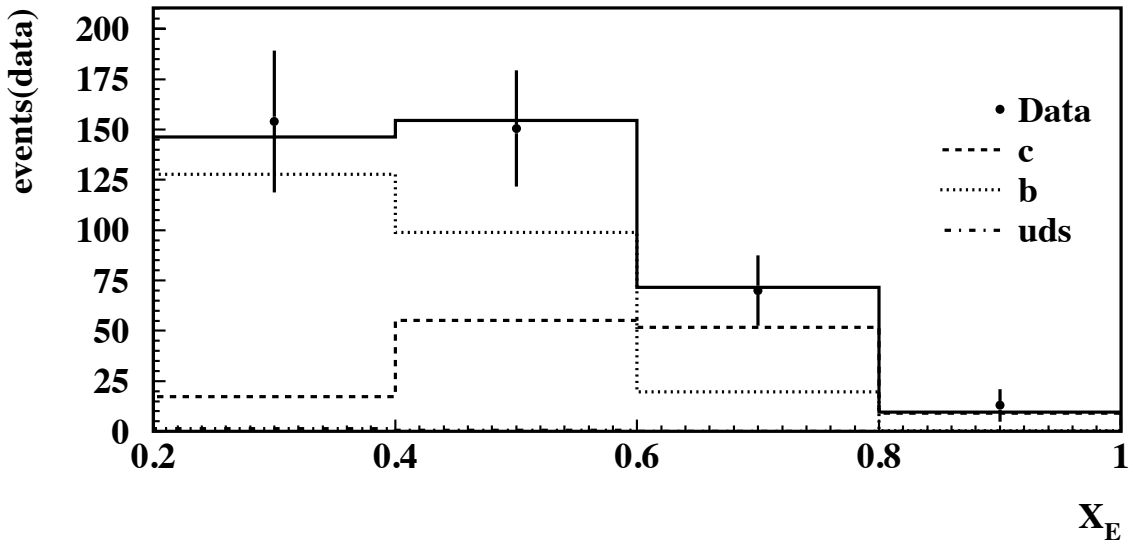

Figure 14: *Background subtracted X_E spectrum for the decay $D_s^+ \to \bar{K}^*(892)K^+$. No efficiency correction is applied. The reconstructed Monte Carlo spectra for $b\bar{b}$ and $c\bar{c}$ events is scaled in order to reproduce the fit results as described in the text.*

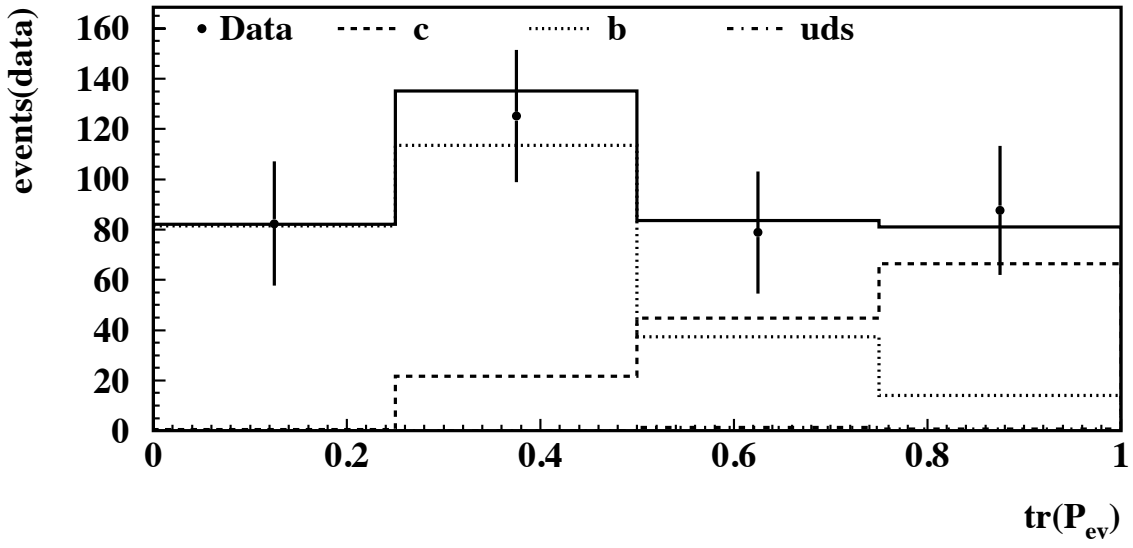

Figure 15: *Background subtracted $tr(\mathcal{P}_{ev})$ spectrum for the decay $D_s^+ \to \bar{K}^*(892)K^+$. No efficiency correction is applied. The reconstructed Monte Carlo spectra for $b\bar{b}$ and $c\bar{c}$ events is scaled in order to reproduce the fit results as described in the text.*

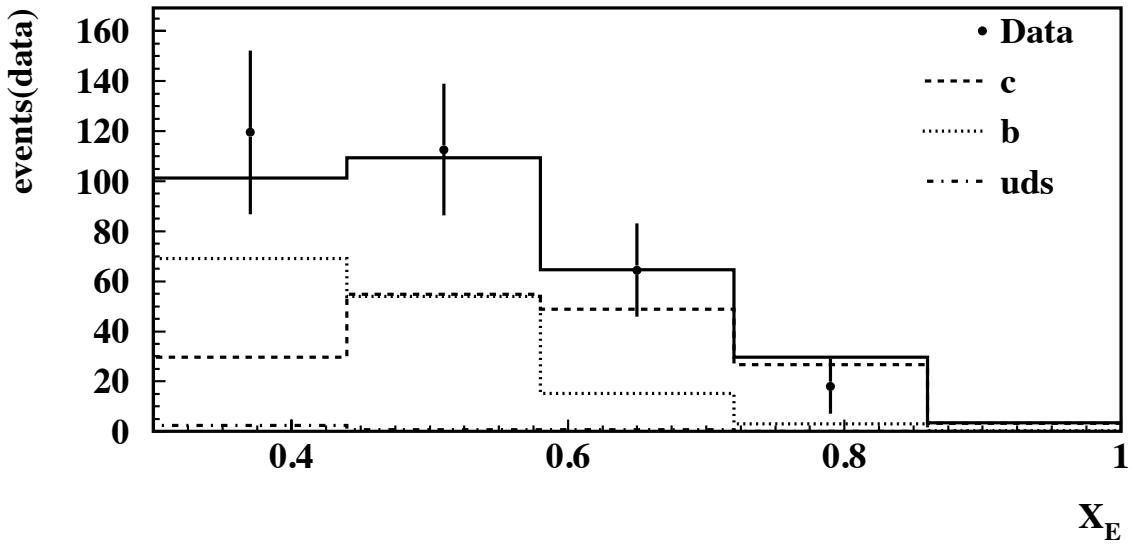

Figure 16: *Background subtracted X_E spectrum for the decay $\Lambda_c^+ \to pK^-\pi^+$. No efficiency correction is applied. The reconstructed Monte Carlo spectra for $b\bar{b}$ and $c\bar{c}$ events is scaled in order to reproduce the fit results as described in the text.*

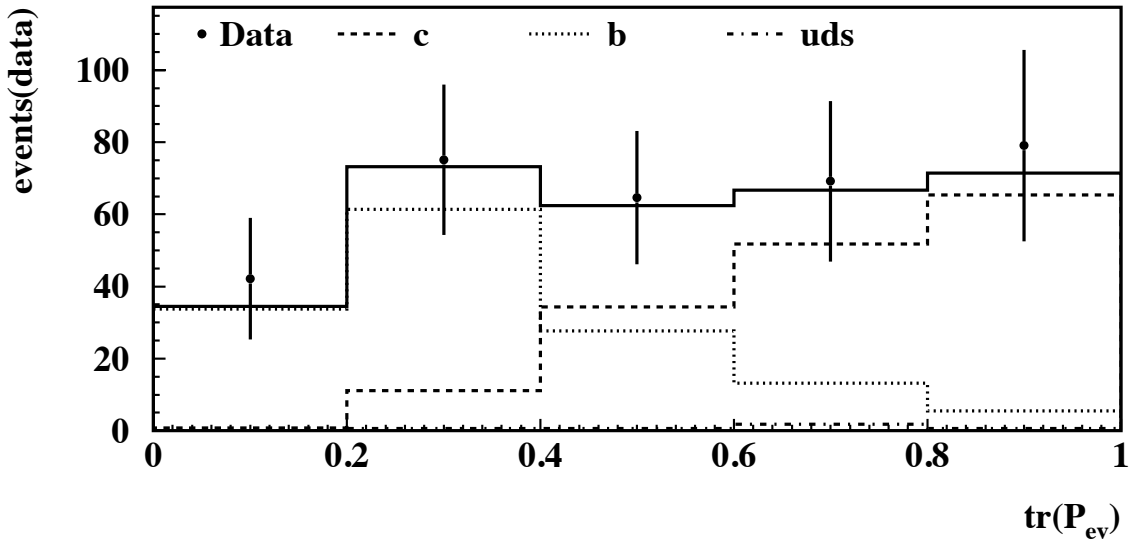

Figure 17: *Background subtracted $tr(\mathcal{P}_{ev})$ spectrum for the decay $\Lambda_c^+ \to pK^-\pi^+$. No efficiency correction is applied. The reconstructed Monte Carlo spectra for $b\bar{b}$ and $c\bar{c}$ events is scaled in order to reproduce the fit results as described in the text.*

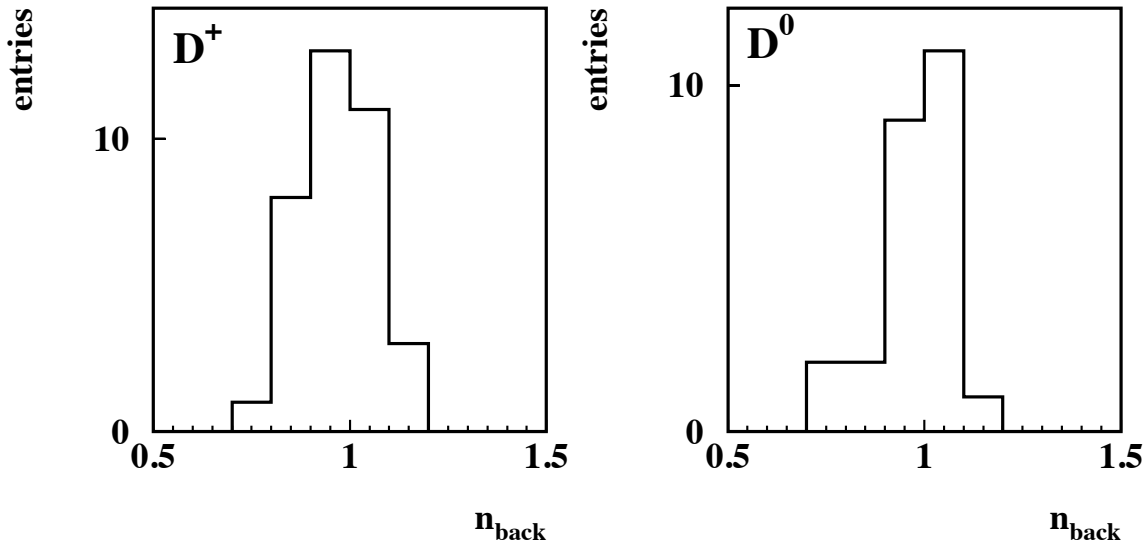

Figure 18: *Background normalisations for the D^+ (left) and the D^0 (right) resulting from the final fit.*

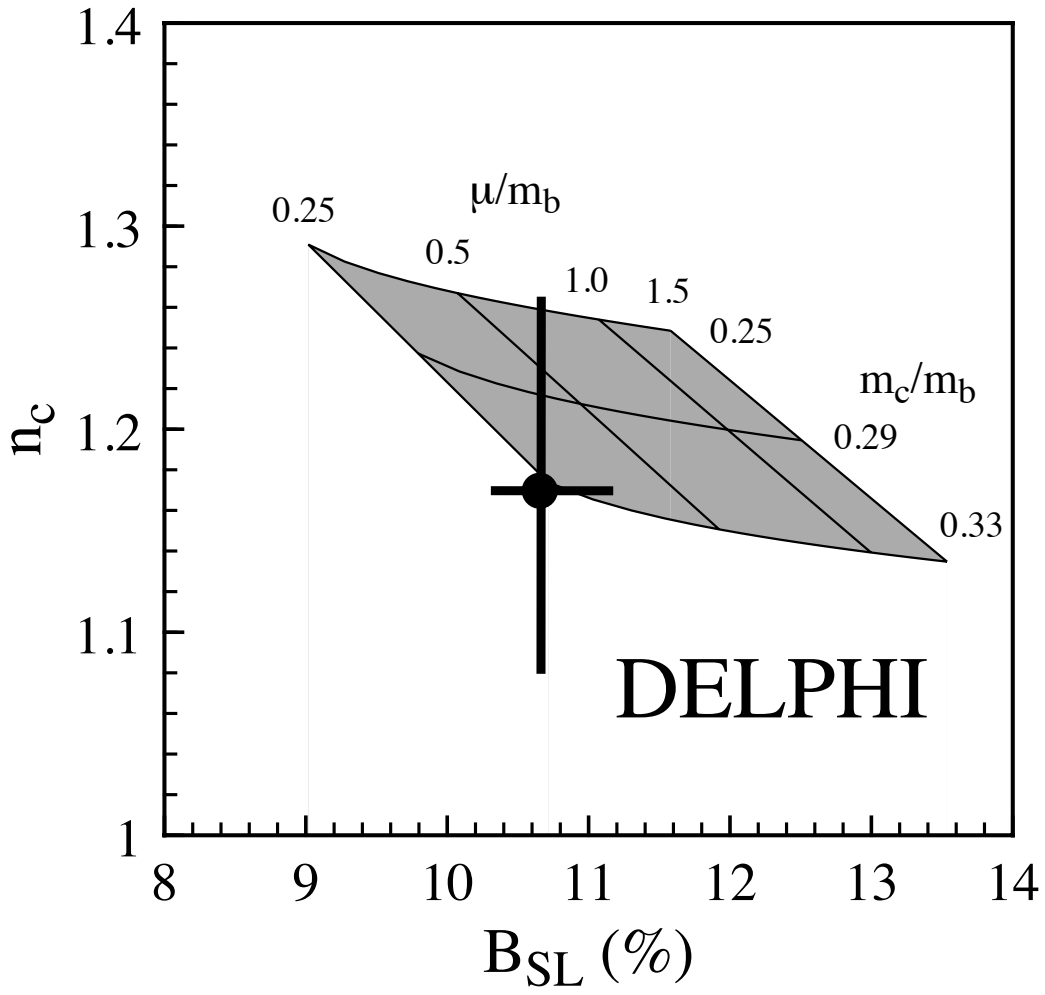

Figure 19: *A comparison of n_c and B_{SL} to the theoretical allowed region [25]. The area is representing the region predicted by theory in the on-shell renormalisation scheme for different values of m_c/m_b and of the renormalisation scale μ/m_b.*